

Interaction of Cd and Zn with Biologically Important Ligands Characterized Using Solid-State NMR and *ab Initio* Calculations

Srikanth S. Kidambi,[†] Dong-Kuk Lee,^{†,‡} and A. Ramamoorthy^{*,†,§}

Department of Chemistry, Biophysics Research Division, and Macromolecular Science & Engineering, University of Michigan, Ann Arbor, Michigan 48109-1055

Received December 19, 2002

For the first time, coordination geometry and structure of metal binding sites in biologically relevant systems are studied using chemical shift parameters obtained from solid-state NMR experiments and quantum chemical calculations. It is also the first extensive report looking at metal–imidazole interaction in the solid state. The principal values of the ¹¹³Cd chemical shift anisotropy (CSA) tensor in crystalline cadmium histidinate and two different cadmium formates (hydrate and anhydrate) were experimentally measured to understand the effect of coordination number and geometry on ¹¹³Cd CSA. Further, ¹³C and ¹⁵N chemical shifts have also been experimentally determined to examine the influence of cadmium on the chemical shifts of ¹⁵N and ¹³C nuclei present near the metal site in the cadmium–histidine complex. These values were then compared with the chemical shift values obtained from the isostructural bis(histidinato)zinc(II) complex as well as from the unbound histidine. The results show that the isotropic chemical shift values of the carboxyl carbons shift downfield and those of amino and imidazolic nitrogens shift upfield in the metal (Zn,Cd)–histidine complexes relative to the values of the unbound histidine sample. These shifts are in correspondence with the anticipated values based on the crystal structure. *Ab initio* calculations on the cadmium histidinate molecule show good agreement with the ¹¹³Cd CSA tensors determined from solid-state NMR experiments on powder samples. ¹⁵N chemical shifts for other model complexes, namely, zinc glycinate and zinc hexaimidazole chloride, are also considered to comprehend the effect of zinc binding on ¹⁵N chemical shifts.

I. Introduction

Several metals such as Zn²⁺, Ca²⁺, Cu²⁺, Hg²⁺, Mn²⁺, and Mg²⁺ are commonly found in living organisms. These ions either act as a structure promoter or play an important role in enzyme activity. A systematic study of the coordination chemistry of metal centers in bioinorganic complexes would be essential to obtain a clear understanding on the role of these metals in several biological and chemical processes. In biosystems such as photosystem-II, phosphotriesterase, calcium, and zinc ion play an important role in the functioning of the protein. A thorough understanding of the properties of these ions could provide valuable information about the activity of these proteins. But the closed d-shell configuration of Zn²⁺ and Ca²⁺ ions makes them unsuitable for spectroscopic techniques such as UV–visible or ESR spectroscopy. Moreover, the properties of these nuclei (low gyromagnetic

ratio and $I > 1/2$) make it a difficult probe to perform NMR experiments. These problems were circumvented using the surrogate probe strategy developed by Vallee and co-workers.¹ Later, this concept of substituting insensitive metal centers with spectroscopic-friendly nuclei was greatly exploited by several research groups² in the field of NMR spectroscopy. All these studies utilized cadmium ion as the NMR probe in elucidating the structure around the metal (mainly Zn²⁺ and Ca²⁺) centers. Cadmium ion occurs in the same group as zinc ion and has a size comparable to both

* To whom correspondence should be addressed. E-mail: ramamoor@umich.edu. Tel: (734) 647-6572. Fax: (734) 615-3790.

[†] Department of Chemistry.

[‡] Biophysics Research Division.

[§] Macromolecular Science & Engineering.

- (1) (a) Coleman, J. E.; Vallee, B. L. *J. Biol. Chem.* **1961**, *236*, 2244. (b) Lindskog, S. *J. Biol. Chem.* **1963**, *238*, 945. (c) Latt, S. A.; Auld, D. S.; Vallee, B. L. *Proc. Natl. Acad. Sci. U.S.A.* **1970**, *67*, 1383.
- (2) (a) Summers, M. F. *Coord. Chem. Rev.* **1988**, *86*, 43. (b) Armitage, I. M.; Pajer, R. T.; Schoot Uiterkamp, A. J. M.; Chlebowski, J. F.; Coleman, J. E. *J. Am. Chem. Soc.* **1976**, *98*, 5710. (c) Ellis, P. D. *Science* **1983**, *221*, 1141. (d) Ellis, P. D. *J. Biol. Chem.* **1989**, *264*, 3108. (e) Rivera, E.; Kennedy, M. A.; Adams, R. D.; Ellis, P. D. *Adv. Magn. Reson.* **1987**, *13*, 257. (f) Jakobsen, H. J.; Ellis, P. D.; Inners, R. R.; Jensen, C. F. *J. Am. Chem. Soc.* **1982**, *104*, 7442. (g) McAteer, K.; Lipton, A. S.; Ellis, P. D. Cadmium-113 NMR. A Surrogate Probe for Zn and Calcium in Proteins. In *Encyclopaedia of Nuclear Magnetic Resonance*; Grant, D. M., Harris, R. K., Eds.; John Wiley & Sons: New York, 1996; Vol. 2, pp 1085–1091 and references cited within.

zinc and calcium ions. The nuclear spin quantum number of $1/2$ for cadmium makes the ^{113}Cd chemical shift an easily measurable NMR parameter, and therefore it is a suitable nucleus to replace Zn^{2+} or Ca^{2+} for NMR studies on biological molecules. Even though Kimblin and Parkin have reported significant differences in the structures of Cd and Zn analogous model complexes,³ this method still seems to be a good starting point to elucidate the structure of Zn-containing biomolecules. Some of the most important benefits in using ^{113}Cd to study the coordination chemistry of metal centers are as follows: (i) it has a large span of ^{113}Cd chemical shift, which allows the characterization of coordination number and type of ligands, and (ii) the chemical shielding tensor elements of ^{113}Cd are sensitive to the chemical environment and provide an easy probe to differentiate metal centers with identical coordination number but different structure (for example: cadmium alaninate and cadmium glycinate).⁴

In many of the metal-containing metalloproteins, the metal centers form discrete units surrounded by various amino acids. To determine the binding nature of the metal, it is necessary to understand the coordination and structural effects of these amino acids on the central atom. These effects are identified either by looking at the metal center or by looking at the ligands, namely, amino acids. It is known that many of the amino acid residues such as glycine, glutamic acid, histidine, cysteine, and aspartic acid in proteins bind to a metal in metalloenzymes. Among them, the most common amino acid that binds to a metal is histidine. Imidazole present in histidine makes it a good complexing agent.⁵ Moreover, imidazole plays an important role in biologically active processes; it works as a proton donor and/or acceptor.⁶ The ability to act as a proton donor was found in the case of triosephosphate isomerase, where it forms a hydrogen bond with the substrate leading to a lower energy for the transition state.⁷ The imidazole moiety also enables charge-transfer processes. One system studied extensively was the oxygen-evolving complex in photosystem II,⁸ which is responsible for the oxidation of water to dioxygen. In this

system, the imidazole moiety of the histidine appears to be bound to the manganese cluster. The other system of importance is phosphotriesterase (PTE).⁹ Cadmium-substituted PTE was found to have two cadmium centers with hexa- and pentacoordination around the cadmium.¹⁰ Both of these centers had two monodentate histidines chelating the central cadmium atom. There are several other metals such as zinc, copper, and iron that bind to the imidazole moiety in histidine present in proteins like alkaline phosphatase^{5a}, plastocyanin,¹¹ and ferredoxins.¹² Thus, examining chemical properties of imidazole, imidazole derivatives, and their metal complexes is essential in understanding the binding nature of imidazole. Further, zinc-containing proteins show three different coordination numbers, 4, 5, and 6, predominantly forming tetracoordinated species¹³ and are influenced by the presence of water. Isotropic chemical shifts and scalar coupling constants obtained from the solution NMR experiments provided some insight about the structure but were not conclusive. To get a better understanding of the structure in rigid metal containing enzymes, NMR experiments should be performed in the solid state. Moreover, chemical shielding anisotropy could provide more information on the nature of coordinating atoms and their positions around the metal. For these reasons, solid-state NMR study of various model zinc and cadmium complexes binding to imidazole and water ligands will be of considerable interest in establishing a relationship between the structure and chemical shift parameters. These NMR parameters, in turn, can be used to characterize the structure at the metal centers in large proteins.

Recently, with the advent of higher magnetic fields and better radio frequency pulse techniques, it is possible to detect zinc directly, which has a spin quantum number $5/2$. Ellis et al. in their latest work exploited cross-polarization and quadruple echo experiments to directly detect different zinc atoms present in zinc formate dihydrate.¹⁴ Using these experiments, they were able to identify the two different Zn atoms present in the crystal structure. In spite of its advantages, direct detection of zinc is expensive and the experimental techniques are technically demanding. Compared to this method, it is relatively easier to determine the change in the chemical shifts of ^{15}N and ^{13}C nuclei present near the metal coordination center as a result of metal coordination. There are few studies in the literature utilizing β,β -[γ - ^{13}C] dideuteriohistidine as a nonperturbing ^{13}C NMR probe of the environments of the histidine residues in a zinc

(3) Kimblin, C.; Parkin, G. *Inorg. Chem.* **1996**, *35*, 6912.

(4) Barrie, P. J.; Gyani, A.; Motevalli, M.; O'Brien, P. *Inorg. Chem.* **1993**, *32*, 3862 and references cited within.

(5) (a) Otvos, J. D.; Browne, D. T. *Biochemistry* **1980**, *19*, 4011. (b) Braun, J.; Schlabach, M.; Wehrle, B.; Kocher, M.; Vogel, E.; Limbach, H. H. *J. Am. Chem. Soc.* **1994**, *116*, 6593. (c) Limbach, H. H.; Hennig, J.; Kendrick, R.; Yannoni, C. S. *J. Am. Chem. Soc.* **1984**, *106*, 4059. (d) Ellis, P. D.; Inners, R. R.; Jakobsen, H. J. *J. Phys. Chem.* **1982**, *86*, 1506.

(6) (a) Strohmeier, M.; Orendt, A.; Facelli, J. C.; Solum, M. S.; Pugmire, R. J.; Parry, R. W.; Grant, D. M. *J. Am. Chem. Soc.* **1997**, *119*, 7114. (b) Ramamoorthy, A.; Wu, C.; Opella, S. J. *J. Am. Chem. Soc.* **1997**, *119*, 10479. (c) Ghanotakis, D. F.; Babcock, G. T.; Yocum, C. F. *Biochim. Biophys. Acta* **1984**, *765*, 388. (d) Nakatani, H. Y. *Biochim. Biophys. Acta* **1984**, *120*, 299. (e) Miyao, M.; Murata, N. *FEBS Lett.* **1984**, *168*, 118. (f) Grove, G. N.; Brudvig, G. W. *Biochemistry* **1998**, *37*, 1532. (g) Debus, R. J. *Biochim. Biophys. Acta* **1992**, *1102*, 269. (h) Chueng, W. Y. *J. Biol. Chem.* **1971**, *246*, 2589. (i) Forsen, S.; Thulin, E.; Drakenberg, T.; Krebs, J.; Seamon, K. *FEBS Lett.* **1980**, *117*, 189.

(7) (a) Munowitz, M.; Buchovchin, W. W.; Herzfeld, J.; Dobson, C. M.; Griffin, R. G. *J. Am. Chem. Soc.* **1982**, *104*, 1192. (b) Bachovchin, W. W. *Biochemistry* **1986**, *25*, 7751. (c) Smith, S. O.; Farr-Jones, S.; Griffin, R. G.; Bachovchin, W. W. *Science* **1989**, *244*, 961. (d) Yufeng, W.; de Dios, A. C.; Mcdermott, A. E. *J. Am. Chem. Soc.* **1999**, *121*, 10389.

(8) (a) Lodi, P. J.; Knowles, J. R. *Biochemistry* **1991**, *30*, 6948. (b) Cleland, W. W.; Kreevoy, M. M. *Science* **1994**, *264*, 1887. (c) Frey, P. A.; Whitt, S. A.; Tobin, J. B. *Science* **1994**, *264*, 1927.

(9) Dumas, D. P.; Caldwell, S. R.; Wild, J. R.; Raushel, F. M. *J. Biol. Chem.* **1989**, *264*, 19659.

(10) Zheng, F.; Zhan, C.-G.; Ornstein, R. L. *J. Phys. Chem. B* **2002**, *106*, 717 and references therein.

(11) (a) Dismukes, G. C. *Chem. Rev.* **1996**, *96*, 2902. (b) Ruttinger, W.; Dismukes, G. C. *Chem. Rev.* **1997**, *97*, 1. (c) Yachandra, V. K.; Sauer, K.; Klein, M. P. *Chem. Rev.* **1996**, *96*, 2927.

(12) (a) Kojiro, C. L.; Markley, J. L. *FEBS Lett.* **1983**, *162*, 52. (b) Chan, T.; Markley, J. L. *Biochemistry* **1983**, *22*, 5982.

(13) Alberts, I. L.; Nadassy, K.; Wodak, S. J. *Protein Sci.* **1998**, *7*, 1700.

(14) Lipton, A. S.; Smith, M. D.; Adams, R. D.; Ellis, P. D. *J. Am. Chem. Soc.* **2001**, *124*, 411 and references cited within.

metalloenzyme alkaline phosphatase^{5a} and ¹⁵N-enriched imidazole ring in porphyrins to understand metal–porphyrin bonding.^{5b–d} These studies clearly showed the ability of ¹³C and ¹⁵N NMR to understand the structure around the metal center.

In this paper, we use cross-polarization and magic angle spinning (CPMAS) NMR spectroscopy to (a) determine the chemical shift anisotropy (CSA) of the cadmium-113 nuclei in cadmium histidinate and cadmium formates, (b) study the effects of metal, both Zn and Cd, on natural abundance ¹⁵N and ¹³C chemical shifts in bis(histidinato)cadmium(II) hydrate and bis(histidinato)zinc(II) hydrate complexes, and (c) determine the ¹⁵N isotropic chemical shifts for [ZnIm₆]Cl₂ and bis(glycinato)zinc(II) hydrate complexes. The results obtained from NMR experiments are correlated with well-characterized X-ray structures.¹⁵ Experimentally determined ¹¹³Cd CSA values for cadmium histidinate are further compared with ab initio values.

II. Experimental Section

Bis(histidinato) M(II) (M = Cd, Zn) Hydrates. L-Histidine was purchased from Fisher Biotech (Fairlawn, NJ), and metal–histidine complexes were prepared using the procedure reported in the literature.¹⁵ In brief, metal carbonate and histidine were mixed in a 1:2 ratio in boiling water. The complexes were extracted and recrystallized in water.

Cadmium Formates. Hydrous cadmium formate was purchased from Aldrich (St. Louis, MO) and recrystallized in boiling water.¹⁶ The anhydrous compound was obtained from the hydrous sample by keeping it in an oven at 140 °C for 2 days.

Bis(glycinato)zinc(II) Hydrate. This sample was purchased from TCI (Portland, OR) and used for NMR studies without further purification.

Zinhexaimidazole Chloride Tetrahydrate. An aqueous solution of imidazole was added to zinc chloride in molecular ratio of 10:1. A trace amount of CuSO₄ was added to this solution. The sample was obtained by slow evaporation as suggested in the crystal structure paper.¹⁷ Further elemental analysis of this complex matched with the expected values.

Solid-State NMR Spectroscopy. All NMR experiments were carried out on a Chemagnetics/Varian Infinity 400 MHz spectrometer operating at resonance frequencies of 400.1, 100.6, 40.5, and 88.7 MHz for ¹H, ¹³C, ¹⁵N, and ¹¹³Cd, respectively at room temperature. A 5 mm double-resonance Chemagnetics MAS probe was used at different spinning speeds ranging from 1.0 to 9 kHz. Cross-polarization (CP)¹⁸ and the TPPM decoupling method¹⁹ were used to improve the sensitivity and resolution of the spectra. Typical 90° pulse widths were 3.5, 4.0, 5, and 3.5 μs for ¹H, ¹³C, ¹⁵N, and ¹¹³Cd, respectively. The rf field strength used for ¹³C/¹H and ¹⁵N/¹H cross-polarization was 35 kHz, and the ¹H decoupling field

strength during the data acquisition was 75 kHz. A 2 ms contact time for CP and a recycle delay of 5 s were used. ¹³C and ¹⁵N chemical shifts were referenced indirectly to adamantane (29.5 and 35.6 ppm) and ammonium sulfate powder sample (24.1 ppm), respectively. For ¹¹³Cd NMR experiments, both static and MAS experiments were performed on bis(histidinato)cadmium(II) complex and cadmium formates in hydrous and anhydrous states. Cadmium formate was used to set up the CP condition. ¹¹³Cd chemical shifts are referenced relative to 0.1 M Cd(ClO₄)₂ (0.0 ppm). Magnitudes of the principal elements of the ¹¹³Cd CSA tensor were determined from the powder spectrum and/or slow spinning spectra using the Herzfeld–Berger sideband analysis program.²⁰ The static powder spectrum was simulated using a FORTRAN-77 program. The principal elements of the chemical shift tensors are represented according to the convention $|\sigma_{33}| \geq |\sigma_{22}| \geq |\sigma_{11}|$.

Ab Initio Calculations. Isotropic and anisotropic chemical shift values of ¹¹³Cd nuclei were calculated using Gaussian98²¹ and utilized density functional theory²² quantum calculation methods. The three-parameter hybrid functional B3PW91²³ with the Kello–Sadlej basis set²³ on cadmium and 6–311+G²³ on the other atoms were used to estimate the ¹¹³Cd CSA values. We showed in our earlier study that theoretical chemical shift values resulting from the above-mentioned method agreed with the experimental values to a reasonable accuracy.²⁴ Initial positional coordinates were obtained from neutron diffraction data.¹⁵ The values were referenced with respect to the experimental isotropic chemical shift determined from the powder spectrum.

Gaussian calculations provide absolute shielding values, and hence the chemical shift values of the complexes were obtained using the equation

$$\sigma(\text{calc}) = -\sigma(\text{complex}) + \sigma(\text{ref})$$

III. Results and Discussion

A. ¹¹³Cd NMR Spectroscopy. (1) Bis(histidinato)cadmium (II) Hydrate, Cd[(C₃H₃N₂)CH₂CH(NH₂)COO]₂. The structure of the bis(histidinato)cadmium(II) hydrate complex is known from the neutron diffraction study.¹⁵ In

- (15) (a) Huess, H.; Bartunik, H. *Acta Crystallogr.* **1976**, *B32*, 2803. (b) Kretsinger, R. H.; Cotton, F. A. *Acta Crystallogr.* **1963**, *16*, 651.
 (16) (a) Post, M. L.; Trotter, J. *Acta Crystallogr.* **1979**, *B35*, 2215. (b) Weber, G. *Acta Crystallogr.* **1980**, *B36*, 1947 (c) Harrison, W.; Trotter, J. *J. Chem. Soc., Dalton Trans.* **1972**, 956.
 (17) (a) Garrett, T. P. J.; Guss, J. M.; Freeman, H. C. *Acta Crystallogr.* **1983**, *C39*, 1031. (b) Lundberg, B. K. S. *Acta Crystallogr.* **1966**, *21*, 901.
 (18) Schmidt-Rohr, K.; Spiess, H. W. *Multidimensional Solid-state NMR and Polymers*; Academic Press: New York, 1994; Chapter 3. Shekar, S. C.; Lee, D. K.; Ramamoorthy, A. *J. Magn. Reson.* **2002**, *157*, 223.
 (19) Bennett, A. E.; Rienstra, C. M.; Anger, M.; Lakshmi, K. V.; Griffin, R. G. *J. Chem. Phys.* **1995**, *103*, 6951.

- (20) Herzfeld, J.; Berger, E. *J. Chem. Phys.* **1980**, *73*, 6021.
 (21) Frisch, M. J.; Trucks, G. W.; Schlegel, H. B.; Scuseria, G. E.; Robb, M. A.; Cheeseman, J. R.; Zakrzewski, V. G.; Montgomery, J. A., Jr.; Stratmann, R. E.; Burant, J. C.; Dapprich, S.; Milliam, J. M.; Daniels, A. D.; Kudin, K. N.; Strain, M. C.; Farkas, O.; Tomasi, J.; Barone, V.; Cossi, M.; Cammi, R.; Mennucci, B.; Pomelli, C.; Adamo, C.; Clifford, S.; Ochterski, J.; Petersson, G. A.; Ayala, P. Y.; Cui, Q.; Morokuma, K.; Malick, D. K.; Rabuck, A. D.; Raghavachari, K.; Foresman, J. B.; Cioslowski, J.; Ortiz, J. V.; Stefanov, B. B.; Liu, G.; Liashenko, A.; Piskorz, P.; Komaromi, I.; Gomperts, R.; Martin, R. L.; Fox, D. J.; Keith, T.; Al-Laham, M. A.; Peng, C. Y.; Nanayakkara, A.; Gonzalez, C.; Challacombe, M.; Gill, P. M. W.; Johnson, B.; Chen, W.; Wong, M. W.; Andres, J. L.; Head-Cordon, M.; Replogle, E. S.; Pople, J. A. *Gaussian 98*, revision A.5; Gaussian, Inc.: Pittsburgh, PA, 1998.
 (22) (a) Kohn, W.; Sham, L. J. *Phys. Rev. A* **1965**, *140*, 1133. (b) Becke, A. D. *J. Chem. Phys.* **1988**, *38*, 2547. (c) Slater, J. C. *Quantum theory of Molecules and Solids. Vol. 4: The Self-Consistent Field for Molecules and Solids*; McGraw-Hill: New York, 1974.
 (23) (a) Becke, A. D. *J. Chem. Phys.* **1988**, *38*, 3098. (b) Lee, C.; Yang, W.; Parr, R. G. *Phys. Rev. B* **1988**, *37*, 785. (c) Perdew, J. P.; Wang, Y. *Phys. Rev. B* **1992**, *45*, 13244. (d) Becke, A. D. *J. Chem. Phys.* **1993**, *98*, 5648. (e) Becke, A. D. *J. Chem. Phys.* **1996**, *104*, 1040. (f) Adamo, C.; Barone, V. *Chem. Phys. Lett.* **1997**, *274*, 242. (g) Kello, V.; Sadlej, A. J. *Theor. Chim. Acta* **1995**, *91*, 353. (h) Clark, T.; Chandrasekhar, J.; Spitznagel, G. W.; Schleyer, P. v. R. *J. Comput. Chem.* **1983**, *4*, 294. (i) Stewart, J. J. P. *J. Comput. Chem.* **1989**, *10*, 209. (j) Raghavachari, K.; Pople, J. A.; Replogle, E. S.; Head-Gordon, M. *J. Phys. Chem.* **1990**, *94*, 5579.
 (24) Kidambi, K. S.; Ramamoorthy, A. *J. Phys. Chem. A* **2002**, *106*, 10363.

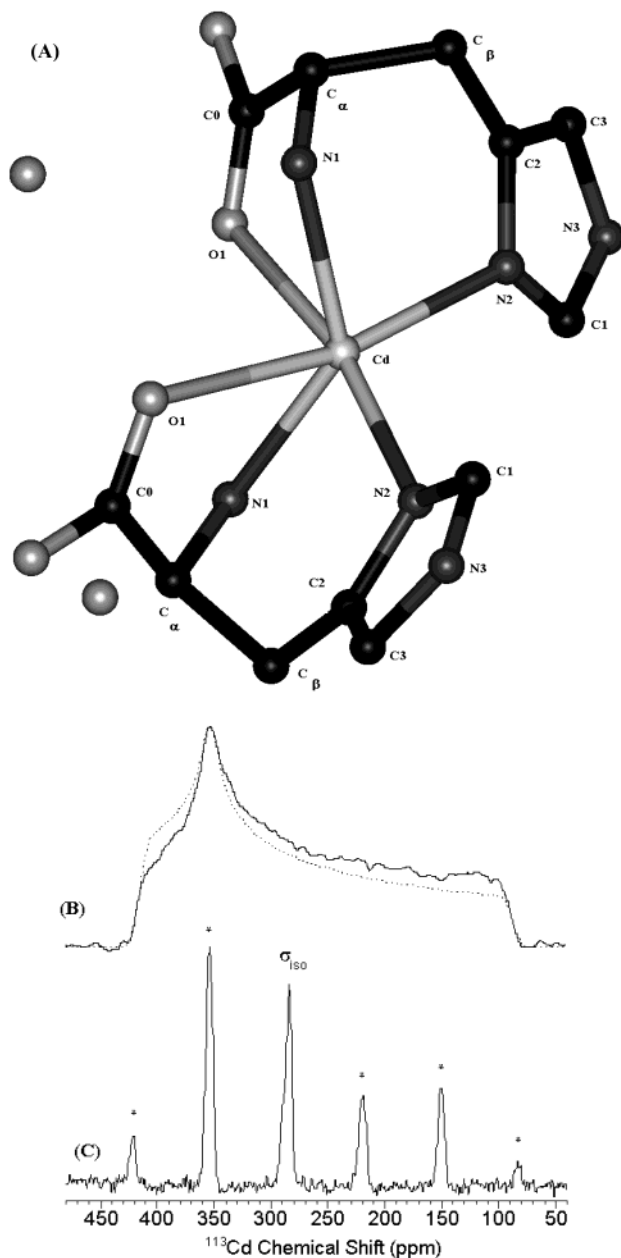


Figure 1. (A) Neutron diffraction structure of cadmium histidinate used in ab initio calculations and also to interpret chemical shifts measured from solid-state NMR experiments. Cadmium-113 chemical shift spectra of bis-(histidinato)cadmium(II) hydrate obtained at static (B) and 6 kHz (C) spinning speeds. The CSA values are determined to be $\sigma_{33} = 416 \pm 3$ ppm, $\sigma_{33} = 354 \pm 3$ ppm, and $\sigma_{33} = 88 \pm 3$ ppm from computer simulation. The simulated spectrum is superimposed onto the static powder spectrum (see dotted line in part B). In part C, asterisks (*) denote spinning sidebands.

this complex, the cadmium center has a distorted octahedral coordination with two histidine ligands chelating cadmium through the imidazolic nitrogen (N2), amino nitrogen (N1), and the carboxylic oxygens (O1) (See Figure 1A.) The histidine complex presented in this work is structurally distinct compared to previously studied cadmium alaninate and cadmium glycinate complexes.⁴ Before starting the discussion on cadmium histidinate, it is useful to present a brief structural comparison between histidine and the other two metal complexes in order to relate the structural dependence of ^{113}Cd chemical shift values. Cadmium gly-

Table 1. Cadmium-113 Isotropic and Anisotropic Chemical Shift Values (ppm) for Cadmium Complexes

compound	σ_{iso}	σ_{33}	σ_{22}	σ_{11}	$\Delta\sigma$
cadmium histidinate					
theory	286	409	348	102	184
static	286 ^a	416	354	88	195
cadmium formate (anhydrous)	-55	-2	-42	-120	79
cadmium formate ^b dihydrate					
Cd1	14.4	45.6	17.4	-18.8	46.3
Cd2	19.9	85.1	30.3	-55.8	97.9
cadmium acetate ^b dihydrate	-53.6	33.5	-69.5	-118.7	127.6
cadmium glycinate ^c	177	445	277	-189	401
cadmium alaninate ^c	177	321	266	-56	216

^a $\sigma_{\text{iso}} = (\sigma_{11} + \sigma_{22} + \sigma_{33})/3$; $\Delta\sigma = [\sigma_{33} - (\sigma_{11} + \sigma_{22})/2]$. ^b Reference 29. ^c Reference 4.

cinatinate consists of a distorted octahedral coordination with two glycine ligands acting as bidentates chelating the central cadmium atom through the nitrogen and oxygen atoms, and the other two coordination sites are occupied by the oxygens of two other glycine ligands, leading to a polymeric structure. In the cadmium-alanine complex, two alanines act as bidentates coordinating the central cadmium atom through oxygen and nitrogen atoms. The two water oxygens also bind to cadmium, leading to an octahedral geometry. Unlike the cadmium glycinate structure, cadmium alaninate forms discrete units with two bidentate alanines arranged in a cis configuration.

Cadmium histidinate discussed in this paper does not form a polymeric structure but forms discrete units, which are linked to the neighboring molecules by hydrogen bondings similar to those in cadmium alaninate. At the same time, the two water molecules present in the cadmium histidinate are not directly bonded to the metal, making it different from the cadmium alaninate. Instead, cadmium histidinate forms very weak intermolecular hydrogen bonds, making each of these units highly distinct.

The ^{113}Cd solid-state NMR spectrum of the cadmium histidinate powder sample was obtained as shown in Figure 1B. The isotropic chemical shift was determined to be 286 ± 3 ppm from the CPMAS spectrum (Figure 1C) of the 6 kHz sample spinning speed and further confirmed by running the experiment at a different spinning speed (data not shown). ^{113}Cd CSA values of cadmium histidinate were determined from simulated static spectrum to be $\sigma_{33} = 416 \pm 3$ ppm, $\sigma_{22} = 354 \pm 3$ ppm, and $\sigma_{11} = 88 \pm 3$ ppm as given in Table 1. The simulated static spectrum is shown as a dotted line superimposed onto the powder spectrum in Figure 1B. The deviation between the simulated (dotted lines) and experimental (solid line) powder patterns in Figure 1B could be attributed to the following sources of experimental errors that were not taken into account in the simulations. Pulse imperfections such as resonance offset and rf field inhomogeneity could reduce the cross-polarization efficiency and hence the S/N of the experimental powder pattern. Since the span of the ^{113}Cd chemical shift powder pattern is large (328 ppm), relative to the strength of the rf field used in the CP experiment, for the bis(histidinato)cadmium(II) hydrate complex, the above-mentioned pulse imperfections might have been the main cause for the mismatch between the simulated and experimental spectra in Figure 1. In addition,

an inefficient decoupling of protons during the signal acquisition could also lead to errors in the measurement of the principal components of the ^{113}Cd CSA tensor. The isotropic chemical shift parameter calculated using the magnitudes of the principal components of CSA, $\sigma_{\text{iso}} = (\sigma_{11} + \sigma_{22} + \sigma_{33})/3$, agreed with the value obtained from MAS experiments. This isotropic chemical shift value differs by approximately 110 ppm compared to the values of the two other amino acid complexes mentioned above and as listed in Table 1. Another complex that has a distorted octahedral Cd^{II} environment with 4N, 2O arranged in a trans configuration is the bis(2-aminomethylpyridine)dinitrato cadmium(II) complex. ^{113}Cd NMR of this complex showed an isotropic chemical shift peak at 222 ppm.²⁵ The difference of 64 ppm between these two cadmium complexes may be attributed to the presence of different aromatic rings (imidazole ring in the former case and pyridine in the latter complex) and hydrogen bonds. However, the isotropic chemical shift values of these two cadmium complexes are much higher (or shifted toward downfield) than the one found in the cadmium complex having similar coordination chemistry but with a cis configuration (52 ppm).²⁶ The exact reason for the effect of configurational differences on chemical shifts is not well established.

The full width at half-maximum (fwhm) of the isotropic peak (Figure 1C) is almost 6 ppm and appears to be a multiplet. This resembles the fine structure seen in the spectra of other amino acids (glycine, alanine)⁴ and imidazole cadmium complexes,²⁷ which were related to the indirect coupling (J -coupling) between ^{113}Cd and two equivalent ^{14}N nuclei. O'Brien and co-workers⁴ rationalized the multiplet pattern for both the amino acid complexes using the expression developed by Olivieri.²⁸ Even though the spectrum of the bis(histidinato)cadmium(II) hydrate sample shows shoulders in Figure 1C, the multiplet pattern is not clearly resolved; this could be due to the presence of two pairs of similar ^{14}N nuclei. A previous study of ^{113}Cd CSA has shown that the anisotropy of the shielding tensor can be correlated with the differences in bond length around the metal center. Also the presence of a water molecule resulted in a large deshielding of the metal.²⁹ Honkonen and Ellis²⁹ have suggested empirical rules to account for the orientations of the three principal shielding tensors. According to this rule, (i) the least shielded tensor element is aligned nearly perpendicular to the plane containing water oxygens and for molecules devoid of oxygens, (ii) the most shielded element is perpendicular to the longest Cd–O bond, and (iii) the least shielded element orients to maximize the shortest Cd–O or Cd–N shielding contributions. In the case of cadmium histidinate (Figure 1A), the bond distances for Cd–N(1), Cd–N(2), and Cd–O(1) are 2.287, 2.290, and 2.480 Å,

respectively, and therefore the most shielded element, σ_{11} , should be oriented perpendicular to the carboxylate oxygen–cadmium bond. Predicting the orientation of the least shielded component, σ_{33} , is difficult without single-crystal studies, but we can conclude that it will be dependent on the plane containing the four nitrogen atoms (two imidazolic nitrogens and two amino nitrogens) on the basis of the empirical rules. The magnitudes of the principal elements of the ^{113}Cd CSA tensor were also theoretically calculated on this molecule using density functional theory and found to be $\sigma_{33} = 414$ ppm, $\sigma_{22} = 343$ ppm, and $\sigma_{11} = 102$ ppm. These are in good agreement with the experimental values (see Table 1). The largest difference in the CSA values is seen for σ_{11} (calculated value is 14 ppm downfield to the experimental value). However, this difference is relatively small compared to the cadmium chemical shift span of 900 ppm for various cadmium complexes.

(2) Cadmium Formates. Structures of both hydrous and anhydrous cadmium formates have been determined using X-ray crystallography.¹⁶ Hydrous cadmium formate has an octahedral geometry with two structurally different cadmium sites whereas anhydrous cadmium formate has a hepta-coordinated pseudo-octahedral geometry. Another known molecule, which has a seven-coordinate geometry, is cadmium acetate dihydrate.¹⁶ Figures 2A and 2B show the crystal structures of anhydrous cadmium formate and cadmium acetate dihydrate, respectively. In anhydrous cadmium formate, there are five monodentate formate oxygens [O(1), O(2), O(4), O(5), and O(6)] and one bidentate formate oxygen O(3) and O(7) encompass the central cadmium atom, whereas in cadmium acetate dihydrate, two water oxygens, O(1) and O(2), two pairs of bidentate acetate oxygens, O(3) and O(4) and O(5) and O(7), and a monodentate bridging oxygen, O(6), encompass the central cadmium atom. The biggest difference between the two complexes is the occurrence of directly bonded water oxygens in cadmium acetate dihydrate. This change in structure led us to explore the ^{113}Cd CSA tensor in anhydrous cadmium formate.

Single-crystal solid-state NMR study on hydrous cadmium formate by Honkonen and Ellis²⁹ identified the presence of two distinguishable cadmium sites as well as the orientation of the tensor elements in the two sites. Hence, we will emphasize the results for the anhydrous complex in this article. TGA analysis on cadmium formates showed that hydrous form loses its water and becomes anhydrous above 110 °C.³⁰ For the present solid-state NMR study, the hydrous sample was placed in the oven at 140 °C for 2 days to completely remove water.

In order to corroborate and differentiate the presence of two different forms of cadmium formates, ^{113}Cd CPMAS spectra for both hydrous and anhydrous forms were collected at the sample spinning speed of 6.5 and 3.5 kHz as shown in Figures 2C and 2E, respectively. The spectra resulted in one sharp isotropic peak at -55 ± 3 ppm from the anhydrous sample (minor peak at -75 ppm may be due to some other

(25) Griffith, E. A. H.; Li, H.; Amma, E. L. *Inorg. Chim. Acta* **1988**, *148*, 203.

(26) Rodeseiler, P. F.; Charles, N. G.; Griffith, E. A. H.; Lewinski, K.; Amma, E. L. *Acta Crystallogr.* **1986**, *C42*, 538.

(27) Rivera, E.; Kennedy, M. A.; Adams, R. D.; Ellis, P. D. *J. Am. Chem. Soc.* **1990**, *112*, 1400.

(28) (a) Olivieri, A. C. *J. Magn. Reson.* **1989**, *81*, 201. (b) Olivieri, A. C.; Hatfield, G. R. *J. Magn. Reson.* **1991**, *94*, 535.

(29) Honkonen, R. S.; Ellis, P. D. *J. Am. Chem. Soc.* **1984**, *106*, 5488.

(30) Abousekkin, M. M.; Morsi, S.; Elgeassy, A. A. *Thermochim. Acta* **1985**, *91*, 1.

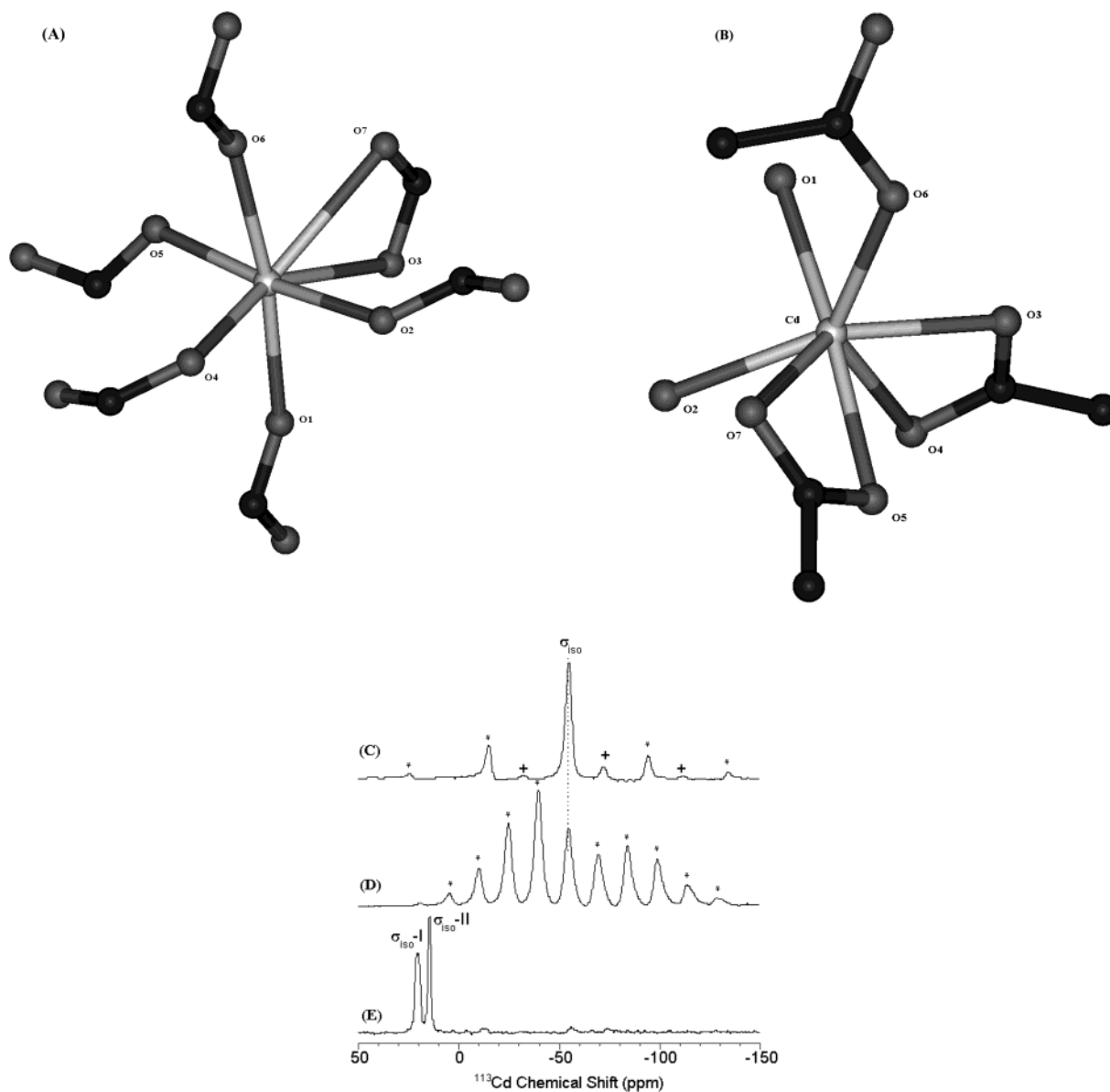


Figure 2. Crystal structures of (A) anhydrous cadmium formate and (B) cadmium acetate dihydrate. Cadmium-113 CPMAS spectra of anhydrous cadmium formate spun at 3.5 kHz (C) and 1.3 kHz (D) and hydrous cadmium formate spun at 6.5 kHz (E). One thousand transients obtained from ≈ 50 mg of powder sample were coadded for each spectrum. Asterisks (*) denote the spinning sidebands. Plus signs (+) designate peaks of an impurity or a different form in the sample and its spinning sidebands.

form of anhydrous cadmium formate) contrasting to two peaks at 14.4 and 19 ppm seen in the hydrous form. Although it is difficult to generalize coordination chemistry with chemical shifts, Rodeseiler and Amma³¹ have proposed that cadmium chemical shifts between -30 and -100 ppm indicate a coordination number greater than 6. On the basis of this rule, we can deduce the presence of seven-coordinated cadmium center in the anhydrous cadmium formate. The magnitudes of the three shielding tensor elements were found to be $\sigma_{33} = -2 \pm 3$ ppm, $\sigma_{22} = -42 \pm 3$ ppm, and $\sigma_{11} = -120 \pm 3$ ppm using Herzfeld–Berger spinning sideband analysis of the 1.3 kHz spectrum (Figure 2D). Magnitude of the most shielded element, σ_{11} , for the anhydrous cadmium formate is similar to that of cadmium acetate. The other two

components, σ_{22} and σ_{33} , differ by 28 ppm (upfield) and 34 ppm (downfield), respectively, from that of cadmium acetate dihydrate values ($\sigma_{33} = 33.5$ ppm; $\sigma_{22} = -69.5$ ppm)^{29,32} as given in Table 1. The difference in the chemical shielding values between these two complexes is small compared to the cadmium chemical shift span of 900 ppm as mentioned earlier. This correlation in NMR parameters can be linked to the bond distances for the seven Cd–O bonds as listed in Table 2. In the case of cadmium acetate dihydrate, bond distances range between 2.294 and 2.597 Å and between 2.259 and 2.599 Å in anhydrous cadmium formate. Two of the longest bonds seen in both the structures are from bidentate formate (O3 and O7 in Figure 2A) and acetate ligands (O3 and O7 in Figure 2B). Also, two oxygens from

(31) Rodeseiler, P. F.; Amma, E. L. *J. Chem. Soc., Chem. Commun.* **1982**, 182.

(32) Ganapathy, S.; Chacko, V. P.; Bryant, R. G. *J. Chem. Phys.* **1984**, *81*, 661.

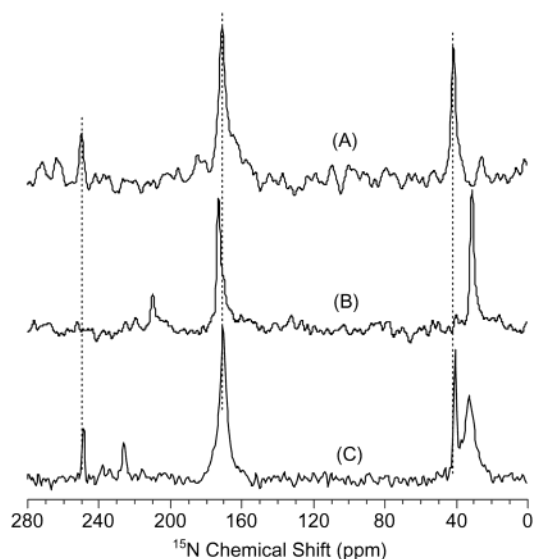


Figure 3. Natural abundance CPMAS ^{15}N chemical shift spectra of (A) histidine, (B) zinc histidinate, and (C) cadmium histidinate. The spinning speed was 7 kHz. Ten thousand transients obtained from ≈ 50 mg of powder sample were coadded for each spectrum.

Table 2. Cd–O Bond Distances (Å) from Cadmium Formate (Anhydrous) and Cadmium Acetate Compounds

	O1	O2	O3	O4	O5	O6	O7
cadmium acetate	2.299	2.325	2.546	2.303	2.294	2.296	2.597
cadmium formate (anhydrous)	2.285	2.323	2.586	2.303	2.259	2.275	2.599

each water molecule (O1 and O2 in Figure 2B) in cadmium acetate dihydrate have distances of 2.299 and 2.325 Å similar to that of the two formate oxygens (2.285 and 2.323 Å). Therefore, the minor difference in the shielding values may be due to the presence of directly coordinated water molecules in cadmium acetate dihydrate and the absence of water molecules in cadmium formate. Now coming to the analysis of the orientation of the shielding elements, σ_{11} should be orthogonal to the longest Cd–O(4) bond based on the previously mentioned empirical rules. But the prediction process for the other shielding components is more difficult due to the absence of water molecules and the presence of five monodentate formates in anhydrous cadmium formate.

B. ^{15}N NMR of Metal–Histidine and Metal–Imidazole Complexes. A commercial L-histidine sample was used for preparing the metal (Zn, Cd) complexes as mentioned in the Experimental Section. ^{15}N chemical shifts of the three nitrogens in histidine are highly dependent on the protonation state and tautomerism,⁶ whereas in metal complexes the presence of coordinate bonds between imidazolic nitrogen and the metal prevents the formation of tautomers avoiding complications during interpretation of NMR spectra. Natural abundance solid-state ^{15}N CPMAS spectrum of the histidine sample resulted in three peaks at 41.2, 249.5, and 170.8 ppm (Figure 3A) accounting for the three nitrogens, namely, (N1) amino nitrogen, (N2) imidazole nitrogen, and (N3) imidazole nitrogen, respectively. These values match with those available in the literature.^{7d}

Table 3. Nitrogen-15 Isotropic Chemical Shift Values (ppm) of Histidine and Imidazole for Free and Metal-Bound (Cd, Zn) Complexes Obtained Using CPMAS Experiments^a

compound	N1	N2	N3
His ^b	41.2	249.5	170.8
His ^c		249.8	171.6
imidazole ^d		248.0	172.2
Cd–His	33.0	226.3	170.8
Zn–His	31.5	210.4	173.5
ZnIm ₃ Cl ₂		232.5	176.8

^a All values are indirectly referenced relative to NH_3 (0.0 ppm) by setting ammonium sulfate at 24.1 ppm. ^b Present result. ^c Literature data.^{7d} ^d References 36 and 37.

The effect of metal–histidine interaction on ^{15}N chemical shifts is studied by performing CPMAS experiments on both zinc histidinate complexes and cadmium histidinate. In the zinc histidinate spectrum (Figure 3B), the influence of coordinate bonds on isotropic chemical shifts is prominent with an upfield shift of 40 ppm for the imidazolic nitrogens (N2) and 9.7 ppm for the amino nitrogens. The upfield shift is related to the shielding effect caused by the presence of the metal atom. The (N3) nitrogen of the zinc complex shifts downfield from 170.8 to 173.5 ppm. Similarly, in the cadmium histidinate spectrum (Figure 3C), the isotropic chemical shift value of the imidazolic nitrogen (N2) changed from 249.5 to 226.3 ppm, an upfield shift of 23 ppm, whereas the amino nitrogen value shifted from 41.2 to 33 ppm, an 8 ppm upfield shift. The isotropic chemical shift of the other imidazole nitrogen (N3) remained unaffected by the cadmium histidinate complex formation. Unlike the zinc histidine spectrum, the isotropic chemical shifts of unbound histidine molecules are seen in the cadmium histidine spectrum, and this is confirmed by the ^{13}C CPMAS spectrum shown later. All these values are given in Table 3. The line width of the metal complexes increases compared to the unbound histidine molecule and may be related to longer T_2 relaxation. (See the amino nitrogen peak at 33 ppm in cadmium histidine complex in Figure 3.) Other studies in the literature reported the influence of pH on the chemical shifts of imidazole and histidine in solution.⁶ These reports demonstrated that a lowering of pH resulted in an upfield diamagnetic shift for the N1 nitrogen caused by protonation of the imidazolic nitrogens and removal of the hydrogen from the imidazole group at a higher pH led to downfield paramagnetic shifts for both of the nitrogens in the imidazole group, but the effect was less prominent on the N3 nitrogen.³³ On the other hand, ^{15}N chemical shifts of doubly labeled [^{15}N]imidazole in metal complexes permitted evaluation of Zn(II) complex formation in homogeneous solution. In solution of Zn^{2+} and imidazole, the ^{15}N resonance in [Zn –imidazole]²⁺ complexes is diamagnetically (upfield) shifted by 10–20 ppm relative to neutral aqueous imidazole.³⁴ In the case of Cd–imidazole complexes, coordination to Cd^{2+} produced an observed 8–12 ppm diamagnetic shift in the ^{15}N resonance of imidazole relative to neutral aqueous imidazole.³⁵ Our solid-state NMR

(33) Blomberg, F.; Rüterjans, H. *Nucl. Magn. Reson. Spectrosc. Mol. Biol.* **1978**, 231.

(34) Mohammed, A., Jr.; Morgan, L. O.; Wageman, W. E. *Inorg. Chem.* **1978**, 17, 2288.

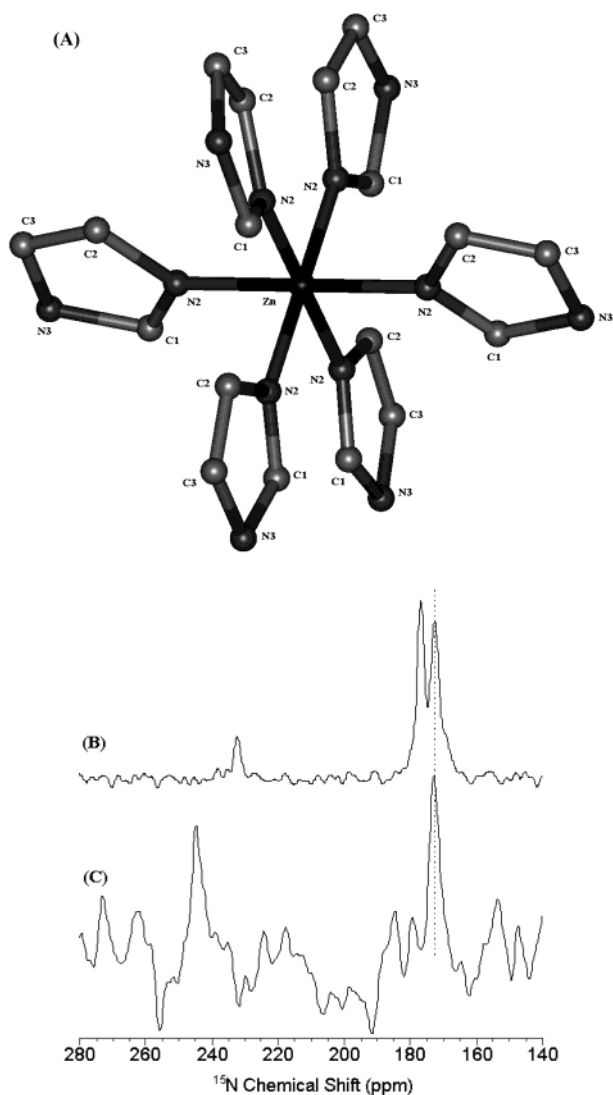


Figure 4. (A) Crystal structure of hexaimidazolezinc(II) chloride. Natural abundance CPMAS ^{15}N chemical shift spectra of (B) hexaimidazolezinc(II) chloride and (C) imidazole. The samples were spun at 7 kHz. Ten thousand transients obtained from ≈ 50 mg of powder sample were coadded for each spectrum. A recycle delay of 60 s was used for imidazole doped with 1% CuSO_4 .

results agree with those obtained earlier in solution.^{33–35} From the current and earlier studies, we can infer that attachment of metal (Zn, Cd) to imidazolic nitrogen leads to an upfield diamagnetic shift irrespective of the physical state. The greater shift of imidazolic nitrogen (N2) and amino nitrogens (N1) in the zinc complex can be accounted for by shorter bond distance between metal and nitrogen (Zn–N1, 2.041 Å; Cd–N1, 2.290 Å; Zn–N3, 2.049 Å; Cd–N3, 2.287 Å).

Zinc has the ability to form both tetrahedral and octahedral complexes¹⁷ with imidazole. The complex considered in this study is ZnIm_6Cl_2 , and the structure is shown in Figure 4A. In ZnIm_6Cl_2 , the central Zn atom is bonded to six imidazolic nitrogens leading to an octahedral symmetry around the metal. Natural abundance ^{15}N CPMAS spectrum (see Figure 4B) of the hexaimidazole complex led to an upfield shift of 15 ppm for the N2 nitrogen relative to the chemical shift

(35) Mohammed, A., Jr.; Wageman, W. E.; Morgan, L. O. *Inorg. Chem.* **1978**, *17*, 3314.

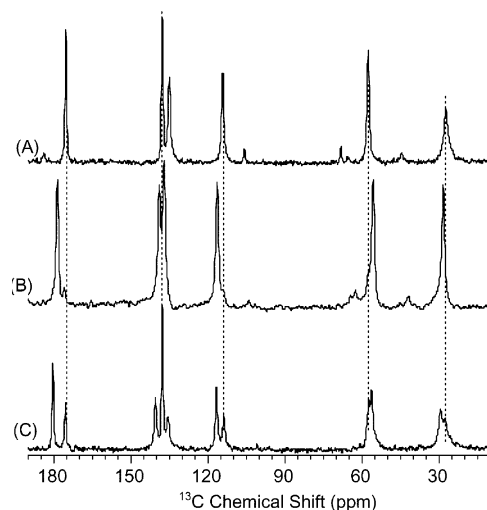


Figure 5. Natural abundance CPMAS ^{13}C chemical shift spectra of (A) histidine, (B) zinc histidinate, and (C) cadmium histidinate. The spinning speed was 7 kHz. One thousand transients obtained from ≈ 50 mg of powder sample were coadded for each spectrum.

value of the solid imidazole sample. Moreover two peaks are seen for the N3 nitrogens. The first peak is shifted downfield to 176.8 ppm from 172.2 ppm relative to free imidazole (values given in Table 3),^{36,37} resembling the trend seen in the zinc histidinate, whereas the second peak occurs at 172.6 ppm, which may be due to some unbound imidazole. To identify this peak, we ran an experiment on a solid imidazole sample doped with 1% CuSO_4 and observed two peaks for the two imidazolic nitrogens (N2, N3) at chemical shift values similar to previously reported data.^{36,37} The S/N ratio for this sample was found to be much lower than that for the hexaimidazole complex, and this is due to a very long T_1 for the imidazole sample as known in the literature.^{36,37} The recycle delay used for the imidazole sample was 60 s even after it was doped with 1% CuSO_4 whereas the recycle delay for the zinc–imidazole complex was 5 s. On the basis of these two spectra, we guess that the second N3 peak seen in the metal–imidazole complex is due to unbound imidazole. Another perplexing aspect was the absence of the N2 nitrogen peak arising from unbound imidazole in this spectrum. This could be related to the longer T_1 for unbound imidazole as mentioned above, and also the absence of hydrogen near the N2 nitrogen may lead to inefficient transfer of magnetization from ^1H to ^{15}N in the CPMAS experiment. As we are concerned more about the effect of metal interaction on the chemical shift of the zinc-bound N2 imidazolic nitrogen, which was clearly identified by a distinct upfield change in the chemical shift from 248 ppm for unbound imidazole to 232.5 ppm using our experiment, we did not analyze the reason for the absence of the unbound imidazolic N2 nitrogen peak.

C. ^{13}C NMR of Metal–Histidine Complexes. Figure 5 shows the natural abundance ^{13}C CPMAS spectra of histidine

(36) Solum, M. S.; Altmann, K. L.; Strohmeier, M.; Berges, D. A.; Zhang, Y.; Facelli, J. C.; Pugmire, R. J.; Grant, D. M. *J. Am. Chem. Soc.* **1997**, *119*, 9804.

(37) Hickman, B. S.; Mascal, M.; Titman, J. J.; Wood, I. G. *J. Am. Chem. Soc.* **1999**, *121*, 11486.

Table 4. Carbon-13 Isotropic Chemical Shift Values of Histidine (ppm) for Free and Metal-Bound (Cd, Zn) Histidine Complexes Obtained Using CPMAS Experiments^a

compound	C1	C2	C3	C _β	C _α	C0
His	137.8	135.2	114.3	27.3	57.6	175.4
Cd–His	140.5	135.7	116.8	29.5	56.3	180.5
Zn–His	139.0	137.1	116.4	28.2	55.5	178.6

^a All values are indirectly referenced relative to TMS by setting adamantane at 29.5 and 35.6 ppm.

(Figure 5A) and its metal complexes (zinc, cadmium histidinates in Figures 5B and 5C, respectively). A histidine molecule has six chemically distinct carbons, and the ¹³C CPMAS spectrum obtained at 7 kHz spinning speed shows clearly resolved isotropic peaks for all the carbons. The ¹³C CPMAS spectra of histidines bound to zinc ions also show highly resolved isotropic chemical shift peaks with altered chemical shift values due to the metal ion interactions. The cadmium histidinate spectrum shows highly resolved ¹³C peaks for both bound and unbound histidines (Figure 5C). This is consistent with the ¹⁵N CPMAS spectrum seen in Figure 3C. The presence of peaks from both bound and unbound histidines was helpful in understanding the effect of cadmium on the ¹³C chemical shifts. Two isotropic chemical shift peaks for the carboxylate carbon in the cadmium histidinate sample occurred at 175.4 and 180.5 ppm (Figure 5C), where the former is for unbound histidine and the latter in the downfield region is due to coordination between cadmium and carboxylate oxygen. It is also seen from Figure 5C that isotropic chemical shifts of C1, C2, C3, and C_β carbons move downfield due to the interaction of the metal with histidine, whereas the chemical shift of C_α carbons lying adjacent to the carboxylate carbons shifts upfield. These effects are also seen in the zinc histidinate with the downfield-shifted carboxylate peak occurring at 178.5 ppm. ¹³C chemical shift values for both unbound and metal-bound histidine are given in Table 4. The results match with the previous studies reported by Couves et al. on zinc–histidine complexes in solution.³⁸ Using titration curves, they showed that ¹³C signals of carboxylate carbon shifted downfield from 175 to 183 ppm upon coordination of varying ratios of histidine to the zinc center.

D. ¹⁵N NMR of Zinc Glycinate. To further see the effect of metal and ligand interaction in biologically relevant molecules, ¹⁵N CPMAS experiments were performed on glycine and zinc glycinate powder samples. X-ray crystallography on Zn–glycine complex³⁹ showed the presence of coordinate bonding between amino nitrogen and the zinc atom. On the basis of the metal–histidine study, it is expected that the binding of metal to amino nitrogen of glycine should lead to an upfield shift relative to that of the free glycine chemical shifts. As anticipated, spectra shown in Figures 6A & 6B for glycine and zinc glycinate samples, respectively, clearly show the change in the chemical shift

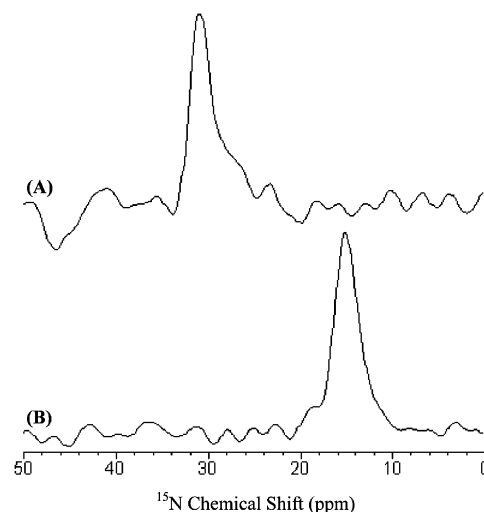


Figure 6. Natural abundance CPMAS ¹⁵N chemical shift spectra of (A) glycine and (B) zinc glycinate. The samples were spun at 7 kHz. One thousand transients obtained from ≈50 mg of powder sample were coadded for each spectrum.

from 30.1 ppm for the amino nitrogen of unbound glycine to 15.1 ppm for the zinc–glycine complex.

IV. Conclusions

This paper illustrates the importance of cadmium chemical shift tensors in model biological complexes. The ¹¹³Cd solid-state NMR experimental data show an upfield shift of 286 ppm for bis(histidinato)cadmium(II) hydrate and a downfield shift of –55 ppm for anhydrous cadmium formate relative to cadmium perchlorate. Also, cadmium histidinate has a CSA span of 330 ppm, which is smaller than the cadmium glycinate and cadmium alaninate complexes. Moreover, the calculated chemical shift values using density functional theory matched well with the experimental data. The marked difference in the chemical shift values for the cadmium histidinate and bis(2-aminomethylpyridine) dinitrato cadmium(II) complexes shows that cadmium chemical shifts are influenced not only by the neighboring ligand atoms but also by bond distances and other secondary effects. In the case of cadmium formates, the effect of different coordination number and the presence of water on the cadmium chemical shift values was clearly seen by the upfield cadmium chemical shift values for anhydrous cadmium formate compare to dihydrate (14.4 and 19 ppm for cadmium formate dihydrate; –55 ppm for anhydrous cadmium formate). Along with the chemical shift of cadmium nuclei, ¹³C and ¹⁵N chemical shifts also provided useful information on the histidine and imidazole complexes. Bonding of nitrogens N1 and N3 and the carboxylate oxygen shifted the chemical shift values upfield and downfield, respectively, relative to unbound histidine. Further, ¹⁵N NMR data on zinc glycinate clearly reflected diamagnetic upfield shifts similar to that of histidine nitrogens. These data indicate that ¹¹³Cd, ¹⁵N, and ¹³C NMR are all useful nuclei to probe metal centers in intermediates or in biologically potent molecules. Availability of ultrahigh magnetic fields (ca. 900 MHz) and a plethora of higher resolution multidimensional solid-state NMR

(38) Couves, L. D.; Hagne, D. N.; Moreton, A. D. *J. Chem. Soc., Dalton Trans.* **1992**, 217.

(39) (a) Newman, J. M.; Bear, C. A.; Hambley, T. W.; Freeman, H. C. *Acta Crystallogr.* **1990**, C46, 44. (b) Low, B. W.; Hirshfeld, F. L.; Richards, F. M. *J. Am. Chem. Soc.* **1959**, 81, 4412.

Interaction of Cd and Zn with Biologically Important Ligands

techniques would enable experimental analysis of ^{113}Cd CSA tensors from a variety of biological systems such as metalloproteins and metal-bound RNA. In addition, recovery of CSA tensors under fast magic angle spinning conditions⁴⁰ provides ^{113}Cd CSA tensors from multiple sites of biological complexes. One specific system to be addressed in the future is the coordination around the active sites in phosphotriesterase. Solution NMR has shown two cadmium chemical shifts at 116 and 212 ppm, but the exact structure is uncertain. As an extension of this work, we are currently working on

(40) Wei, Y.; Lee, D. K.; McDermott, A. E.; Ramamoorthy, A. *J. Magn. Reson.* **2002**, *158*, 23.

model complexes to find out the exact structure around these metal sites using both experiments and ab initio calculations.

Acknowledgment. This study was supported by the research funds from the National Science Foundation (CA-REER development award to A.R.). We thank Dr. Colaneri for his suggestions on the preparation of cadmium histidinate complex, Dr. Rajendiran for useful comments on the manuscript, and Manolis from Dr. Pecoraro's lab for help with the figures.

IC026287D